Exploration of Different Models And Photoelectric Properties of A-Si-H P-I-N Photo Sensor

Dilip Kumar Jalan
Research scholar , Central Dept. of physics. LNM, university Darbhanga
Associate professor , P.K. Campus, Kathmandu (Nepal)

Abstract: Compared to crystalline silicon and polycrystalline silicon, amorphous silicon (a-Si) is preferred because of its excellent characteristics such as high absorption coefficient, good response in low-light environment, and cheap photo sensor material. The inherent disorder of the material creates many charge defect states that hinder carrier transport. Charging defects in the optically active material, the intrinsic layer (I layer) of a-Si: H PIN photodiodes, reduce the built-in electric field, thereby increasing the local light absorption coefficient and reducing the free light average lifetime Career. Improves responsiveness and sensitivity while reducing response time. Short-distance optical communication, optical storage systems, active pixel sensors, and imaging sensors require the high responsiveness and sensitivity of low dark current optical sensors. The p-i-n a-Si: H photodiode is a promising device. Natural and light-induced local densities and energy distributions in the energy gap of a-Si: H have a significant effect on the photoconductivity of thin film photodiodes. It has been observed that deep defect states in the i layer contribute to capacitance at various bias voltages. In addition, capacitors reach an upper limit close to the built-in potential. Based on this method and the results obtained, a-Si: H p-i-n photodiodes were used as biosensor transducers to detect chemiluminescence in mammalian cells.

Keywords- Amorphous Silicon, Photodiode, Biosensor Transducer, Intrinsic Layer, Photoconductivity

I. Introduction

Lithography-based micro technology, originally used to implement integrated semiconductor structures for microelectronic chips, is rapidly being applied to produce microsystem devices suitable for a variety of applications. In particular, the introduction of the microanalysis system (μTAS) concept and the development of the micro-electromechanical system (MEMS) have made the development of an on-chip laboratory (LOC) system a powerful tool for bio-molecular analysis. For real-time applications, the LOC device is an example of a system that allows for lab functions that are typically lab-scale, have low response time, low sample consumption, and field operation due to the high level of miniaturization. While the application of LOC is still novel and conservative, companies and research teams are increasingly interested in many areas such as chemical analysis, environmental monitoring and medical diagnostics. However, there are very few LOCs currently on the market, and in many cases, experimental equipment is required for operation. Therefore, current research integrates microfluidic devices on the same substrate (glass, plastic, crystalline silicon, etc.) with different physical and optical sensors, and includes a single step that includes analysis of the entire sample. Includes manufacturing analysis tools. Preparation, sample processing, analytical testing.

Detection is usually performed using an off-chip detection system that measures the fluorescence emitted by the fluorescent dye attached to the target molecule. Recently, different groups have integrated electrical and / or optical sensors with microfluidics to enable on-chip inspection, increasing system sensitivity and compactness. In particular, optical detection of biomolecules based on organic and inorganic thin film photosensors has been developed. One of the most promising materials for this purpose is hydrogenated amorphous silicon (a-Si: H) and its alloys. The low deposition temperature (below 250 ° C) and its physical properties make it easy to use materials in various devices such as solar cells, electronic switches, strain sensors, and optical sensors. Various research groups have developed the use of thin-film a-Si: H photo-sensors to detect biomolecules, especially in terms of labeling and label-free technology. Recently, the same a-Si: H structure has also been used as a temperature sensor in glass laboratory systems for molecular amplification by polymerase chain reaction (PCR) technology to achieve point monitoring of temperature distribution. This study proposes using a single a-Si: H diode as a multi-parameter sensor to measure temperature and radiant intensity to improve the integration and miniaturization of the LOC system. In particular, considering the fact that temperature changes affect the light response, they scrutinize the requirements that the structure must meet. On the other hand, the measurement value of temperature accuracy may decrease due to changes in light intensity.

II. Background

1. Al Tarabsheh, A. & Akmal, M. (2019) propose contrast to prior art models, hydrogenated amorphous silicon shunt resistance was described as a uniform resistance across the absorber layer (i-layer). The shunt resistance of a-Si: HPV battery is calculated according to this function. A more detailed description of the shunt resistor is provided at the position of the entire i layer. The emission of electron-hole pairs depends on the photon wavelength and the PV cell potential. There is a shunt resistance due to current leakage between the front and back contact layers of the i layer. In their paper, the Poisson equation, continuity equation, and transfer equation are solved at each position of the i layer to calculate the current of electrons and holes and obtain a wide range of potential values. the contribution of electrons and holes to the shunt leak is calculated independently by separating the current density / voltage (J / V) curves of electrons and holes at each position in the i layer. This study shows that the effective value of the position-dependent shunt resistance caused by electrons and holes is equal to the effective shunt resistance of the PV cell calculated by J / V and.

There is a spatial variation of the shunt resistance of a-Si: HPV cells at each position in the i layer. The current density-voltage J / V curve for each charge carrier is calculated by solving the Poisson equation, continuity equation, and transfer equation at each position in the i layer. Since the J / V curves of the two carriers change with the i layer, the shunt leakage current of each carrier changes accordingly. As a result, it is found that the parallel equivalent circuit of the position-dependent shunt resistance caused by electrons and holes is equal to the effective shunt resistance of the PV cell calculated from the complete J / V characteristics. This uses a shunt resistor in the equivalent circuit

of a PV cell consisting of two shunt resistors connected in parallel. One is an electron and the other is a hall. It has also been shown that by increasing carrier mobility, the parallel leakage current of PV cells can be reduced.

2. Adhikari et al.(2019) propose Nanocrystalline hydrogen silicon (nc-Si: H) substrate structure nip solar cells are active absorber layers prepared by plasma enhanced chemical vapor deposition (PECVD) and RF magnetron sputtering on soda-lime glass substrates. Manufacturing. When a cell with a nanocrystalline PECVD absorber and a textured back reflector was used as a baseline for comparison, there was about 6% power conversion efficiency. In contrast, the cell with the sputter absorber achieved an efficiency of about 1%. External quantum efficiency (EQE) simulations were compared with experimental EQEs to determine carrier collection probability gradients for devices with sputtered i-layer absorbers. This incomplete carrier collection at the absorber is most noticeable for materials near the n / i interface, and nc-Si: H is scattered by vacuum damage during sputter absorber layer deposition. The n / i interface is damaged during device fabrication due to excessive deposition of the sputtered i layer. Nip-Si: H devices were prepared using different specific Si: H absorbers using different specific Si: H absorbers. The standard PECVD nc-Si: Hi layer was fully manufactured under vacuum. PECVD nc-Si: Hi layer.

The sample was removed from the vacuum between deposition of the underlying n layer and top p layer, and the sputtered nc-Si: Hi layer had the same vacuum break. To their knowledge, this is the first report of a functional PV device containing a sputtered nc-Si: H absorber layer. Devices with sputter absorbers have lower PCE than devices with PECVD absorbers. The vacuum damage associated with the manufacturing process of the sputter absorber was found to be only about 1% of the absolute decrease in PCE. Further reduction in PCE for sputter absorber based devices is due to volume loss and recombination loss at the interface. The collection probability distribution obtained by comparing the measured values of a device containing a sputtered nc-Si: Hi layer with a simulated EQE is a reduction in carrier collection from the middle to the block i layer, n / i interface. Over sputtered layers of sputtered nc-Si: Hi layers are damaged. These losses are assessed and implemented by performing all depositions within the loadlock system without unnecessary vacuum interruption, ensuring process compatibility and interfacial stability between doped and undoped layer depositions. Will be. Can be reduced. The sputtered material itself needs to be further optimized to achieve a level of performance comparable to that achievable with PECVD.

3. Wang et al. (2018) report proposes a compact hybrid photosensor by vertically integrating an a-Si: H photodiode and a low temperature polysilicon (LTPS) thin film transistor (TFT). Photodiode-gate LTPS TFTs combine sensing, storage, and readout switching functions with internal photoconductive gain to form high-resolution, high-sensitivity, single-transistor active pixel sensors for large area imaging.

4. Maslov et al. (2018). In their paper they present a model for calculating the current-voltage characteristics of a-Si: H / a-SiC: H-based double junction solar cells. The model takes into account the properties of these materials. The IV dependence of solar cells was modeled as a pin structure based on a-Si: H and a-SiC: H. Compare simulation results with experimental results.

5. Xu, Y. et al. (2018) propose achieve low-dose dynamic X-ray imaging, the new active pixel sensor (APS) has a dual-gate low-temperature polycrystalline silicon thin film transistor (LTPS TFT) as the readout TFT, which is vertically controlled by an amorphous silicon pin photodiode. Modeling and simulation TCAD simulation results show that the hybrid integrated sensor has a subthreshold swing (SS) of 0.18 V / decade and a top gate threshold voltage related parameter γ of -1.04. Small SS, Jstrong's phototop dependency, and high fill factor are promising for fast response and high sensitivity flat X-ray detectors.

6. Kim, K. & Kuo, Y. (2017) they investigated the asymmetric sensor transmission mechanism light detection and investigated a-Si: Hp-i-n diodes using devices with different i-layer thicknesses and electro-optic stress methods illuminated with three different wavelengths of light. I layer. The position of photogenerated electrons in a pair of holes depends on the wavelength of the irradiated light, leading to asymmetric transfer and loss of carriers. Therefore, the performance of a-Si: H pin photodiodes is a complex function of wavelength and structural defects.

7. Mohamme et al. (2014) studied on the Shockley-Read-Hall hypothesis, a theoretical model and simulation of the photoelectric characteristics of an a-Si-H PIN photoelectric sensor are presented. The carrier lifetime is simulated using the MATLAB program, and the rate of recombination and generation depends on the thickness of the intrinsic layer (layer I). The effects of intrinsic layer thickness on electron and hole concentration, collection efficiency, and short circuit current density were investigated. As the thickness increases, parameters such as recombination rate, formation rate, internal electric field, electron and hole concentration, carrier lifetime, and short circuit current density all change.

The irregularities inherent in amorphous silicon cause several charge defect states and prevent carrier transport. We know that the energy level of the dangling bond state from shallow to deep is responsible for the characteristic photodiode shape. Shockley-Read-Hall uses a mathematical model to derive an a-Si-H PIN photodiode sensor. When creating mathematical models using MATLAB computer program analysis.

- ✓ Increasing the thickness of one layer increases the concentration and lifetime of photogenerated electrons. The concentration of photogenerated holes gradually decreases to a minimum at a thickness of 400 nm and the lifetime remains nearly constant over a wide range of I layer thicknesses.
- ✓ As the thickness increases, the recombination rate decreases, indicating a minimum thickness near 425 nm.
- ✓ The simulated photogenerated short-circuit current density increases with increasing thickness and saturation exceeds 500 nm.
- ✓ As the I- layer thickness increases, the collection efficiency decreases, especially if the layer thickness is less than 150 nm. This drop is a function of defect density, with higher defect densities being steeper.

8. Jelodarian & **Kosarian (2012)** propose to a-Si: H / a-SiGe: H p- and i-layer characteristics of electrical behavior of thin-film heterostructure solar cells (such as electric field, photogeneration rate, recombination thickness and doping concentration), tested It

was. The introduction of Ge atoms into the Si lattice of Si-based solar cells is an effective way to improve its properties. In particular, the battery current density can be increased without reducing the open circuit voltage of the battery. Optimization has been shown to increase the efficiency of a-Si: H / a-SiGe solar cells by about 6% compared to conventional a-Si: H solar cells for the appropriate Ge concentration. The In this study, a new evaluation and optimization of amorphous silicon double junction (a-Si: H / a-SiGe: H) thin film solar cells to optimize a-SiGe: H gap single-junction solar focusing Propose. The p-layer doping concentration, p-layer and i-layer thickness, and the Ge content of the film are optimized. The maximum efficiency is 23.5%, the short-circuit current density is 267 A / m2, and the open voltage of the double junction solar cell is 1.13 V.

9. Boussettine et al. (2012) propose to thin-film silicon solar cell research needs to consider the electronic structure and optoelectronic properties of different amorphous layers. However, one program that makes sense for this application is AMPS-1D. In this study, AMPS 1D was used to perform computer modeling of a-Si: H / a-SiGe: H tandem solar cells in p-in / pin configuration. Efficiency of amorphous silicon solar cells used as top cells. However, researchers have analyzed this effect, especially in terms of current density and quantum efficiency. They also expressed interest in selecting a-SiC as the window layer rather than a-Si materials. Next, they modeled a series of a-SiGe solar cells as bottom cells and examined the materials that make up the solar cells, especially the interface between a-SiC / a-SiGe interfaces. By properly selecting the tunnel junction, they successfully modeled a tandem a-Si / a-SiGe solar cell, and simulation results showed improved battery performance compared to a single junction . The simulation results are in good agreement with the experimental results. One-dimensional device modeling of tandem a-Si / a-SiGe solar cells using AMPS 1D has been investigated and structural disorder of amorphous materials is taken into account by appropriate models. It is known that the performance of the window layer greatly affects the performance of the solar cell. An 8 nm thick a-SiC window layer shows higher efficiency.

10. Zheng et al. (2012) They propose in their article to discuss low-cost triple-junction solar cells that are important for industrial development. Amorphous silicon / amorphous silicon tandem solar cells, industrial silicon / amorphous silicon / microcrystalline silicon (a-Si: H / a-Si: H / μc-Si: H) using industrially complete single chamber deposition technology Deposition conditions / p-tunnel junction process produced junction solar cells with an initial conversion efficiency of 9.13%, including H plasma treatment, changes in the deposition conditions of the μc-Si: Hn layer, and monolayer p. The layer thickness changes as the room grows. The introduction of single-chamber microcrystalline silicon thin-film solar cell technology has proven to accelerate the development of amorphous silicon thin-film solar cells in the industry.

Low-cost amorphous silicon / amorphous silicon tandem solar cells use a complete single-chamber deposition technology based on acicular microcrystalline silicon solar cell plasma with single-chamber Si: H / a-Si: H deposition Implemented in the industry. Optimized H plasma treatment time, μc-Si: HN layer deposition conditions and μc-Si: HP layer thickness, μ / μc-Si: H PIN type triple junction solar cell n / p tunnel junction process is processed in one chamber. Crystalline silicon / amorphous silicon / microcrystalline silicon triple junction solar cells are 9.13%.

III. Technical Structure

3.1. Sensor Structure

The basic structure of the device is p-type doped amorphous silicon carbide (a-SiC: H) / intrinsic a-Si: H / n-type doped a-Si: H heterojunction. The diodes were deposited by plasma enhanced chemical vapor deposition (PECVD) on a glass substrate covered with a transparent indium tin oxide (ITO) conductive layer. This layer serves as the bottom electrode of the device, and serves as a photo sensor application as a window layer of light that is irradiated onto the photodetector by the glass. Vacuum-deposited Cr / Al / Cr stack structure on a-Si: H diode appears as the top contact of the structure. The SU-8 insulating layer is deposited over the diode to avoid a short circuit between the upper and lower electrodes and reduce the current component caused by the surrounding of the exposed diode.

They manufactured several 2 x 2 mm 2 diodes using standard microelectronic technology. These techniques are arranged in four arrays for physical and chemical vapor deposition of thin films, dry and wet etching of different materials, and geometric patterning. Light.

The device's current-voltage characteristics were evaluated using a Keithley 236 Light Source Measurement Unit (SMU). Delivers 10 -11 A / cm 2 current and small (10 mV) reverse voltage with excellent reproducibility between samples. This value is determined so that the noise current contribution is approximately 2 fA / √Hz. This is lower than the smallest signal that can be detected in the experimental setup.

3.2. Characterization as Radiation Sensor

Due to the optical properties of a-Si: H, p-i-n junctions are widely used as thin film devices for light detection. The active layer of the sensor is an intrinsic layer, and the holes / electrons generated by the absorbed light are swept toward the doped region by the electric field present in the intrinsic region. The doped layer provides a built-in potential at the junction, but does not contribute to the photocurrent because the high-density charged dangling bond defects due to doping of amorphous silicon strongly capture a small amount of photogenerated carriers.

The spectral sensitivity of p-i-n photodiodes can be designed with three layers of light absorption by adjusting the thickness and energy gap. A Device with the energy gaps of p-type, i-type and n-type materials measured with a single layer deposited on Corning glass substrate were equal to 1.92, 1.79, 1.71 eV, respectively, and the thickness was also equal. 10,400 and 200. Every 50 nanometers.

One designed structure achieve maximum response at wavelengths between 400 and 600 nm, and the light sensors are suitable for biochemical applications where chemiluminescent or fluorescent signals need to be detected.

Figure 1(a) shows the quantum efficiency (QY) curve of a photodiode measured in a short-circuit condition. As reported in this mode of operation, ambient leakage current is minimized, so this is the bias condition chosen when using a diode as a radiation sensor.

Features dual arm settings such as tungsten light source, monochromator Spex 340E, beam splitter, calibrated UV

enhanced crystal silicon diode. From this function and the following equation.

$$R = \frac{QY.\lambda.q}{hc}$$

Where λ is the wavelength, q is the electronic charge, h is the Planck constant, and c is the speed of light. The optical sensor responsiveness (R) reported in Figure 1(b) is approximately 280 mA / W at 450 and 600 nm and is shown. The maximum value at 510 nm is 350 mA / W.

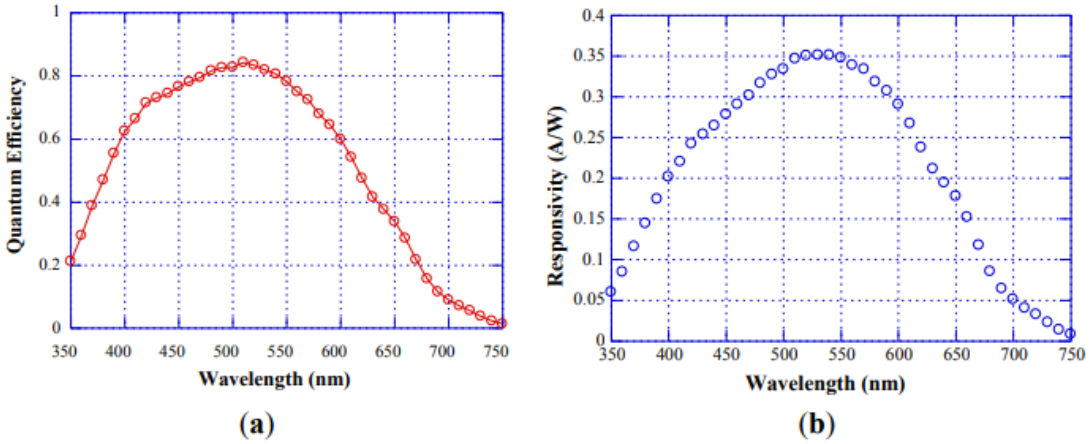

Figure 1. Quantum efficiency (a) and responsively (b) curves of p-i-n a-Si:H photodiode measured in short circuit condition.

3.3. Characterization as Temperature Sensor

The same a-SiC: H / a-Si: H pin diode is described as a temperature sensor that measures the current-voltage characteristics of forward and reverse bias voltage in the temperature range of 30 ° C to 90 ° C. Taken with a probe station equipped with a temperature-controlled chuck, using a thermocouple as the temperature reference. As expected, at constant voltage, the reverse saturation current depends exponentially on temperature under reverse bias conditions, but at constant current, the diode voltage depends on temperature under forward bias conditions. Linearity decreases. These results are summarized in Figure 2. (a) In particular, Figure 2 (a) shows the diode current and temperature for a reverse diode bias of 0.2, 0.6, or 1 V, and Figure 2 (b) shows a positive current of 10. Or through the device 20 nA. As current flows, the diode voltage drop changes with temperature.

Under forward bias conditions, when the bias current exceeds 10 nA, the temperature sensitivity (ST) achieved is equal to 3.2 mV / K, which is greater than the temperature sensitivity (ST) of the crystalline silicon diode. a-Si: H diodes are considered very promising candidates for detecting very small temperature changes in LOC applications.

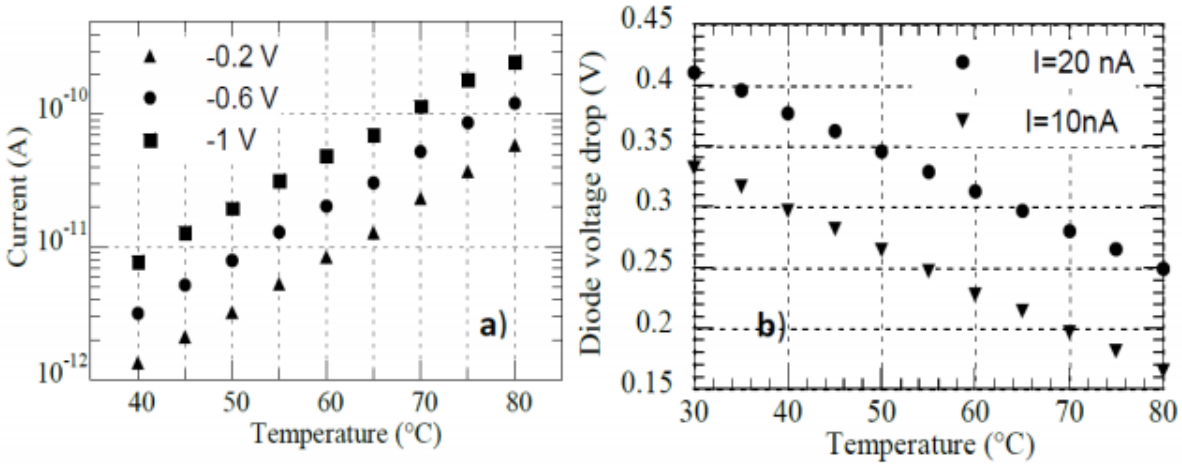

Figure 2. (a) Under reverse voltage bias, the current through the device diode as a function of temperature equals -0.2 V (triangles), -0.6 V (circles) and -1 V (squares). **(b)** The relationship between the voltage drop across the diode and the temperature when the forward current of 10 devices is nA (triangle) or 20 nA (circular symbol)

IV. Conclusion

The p-i-n a-Si: H photodiode is a promising device. Natural and light-induced local densities and energy distributions in the energy gap of a-Si: H have a significant effect on the photoconductivity of thin film photodiodes. It has been observed that deep defect states in the i layer contribute to capacitance at

various bias voltages. In addition, capacitors reach an upper limit close to the built-in potential. Based on this method and the results obtained, a-Si: H pin photodiodes can be used as biosensor sensors to detect chemiluminescence in mammalian cells. Compared to crystalline silicon and polycrystalline silicon, amorphous silicon (a-Si) has excellent characteristics such as a high absorption coefficient, good response in low light environments, and low cost optical sensor materials. The inherent disorder of the material creates many charge defect states that hinder carrier transport. Charging defects in the optically active material, the intrinsic layer (I layer) of a-Si: H PIN photodiodes, reduce the built-in electric field, thereby increasing the local light absorption coefficient and reducing the free light average lifetime Career. Improves responsiveness and sensitivity while reducing response time. Short-distance optical communication, optical storage systems, active pixel sensors, and imaging sensors require the high responsiveness and sensitivity of low dark current optical sensors.

References:

1. Al Tarabsheh, A., & Akmal, M. (2019, April). Calculation of the Shunt Resistance across the Absorber Layer of Hydrogenated Amorphous Silicon Photovoltaic Cells. In *2019 6th International Conference on Electrical and Electronics Engineering (ICEEE)* (pp. 12-16). IEEE.
2. Adhikari, D., Junda, M. M., Grice, C. R., Marsillac, S. X., Collins, R. W., & Podraza, N. J. (2019). nip Nano-crystalline Hydrogenated Silicon Solar Cells with RF-Magnetron Sputtered Absorbers. *Materials*, *12*(10), 1699.
3. Wang, K., Zhou, X., Zhang, M., Xu, Y., Wong, M., & Kwok, H. S. (2018, June). A One-Transistor Active Pixel Sensor Formed by A Vertical Photodiode-Gated Low-Temperature Polysilicon Thin-Film Transistor. In *2018 IEEE International Conference on Electron Devices and Solid State Circuits (EDSSC)* (pp. 1-2). IEEE.
4. Maslov, A. D., Mishustin, V. G., Piryugin, A. V., & Vishnyakov, N. V. (2018, June). Physical model to calculate current-voltage characteristics of double-junction solar cells based on a-Si: H and a-SiC: H. In *2018 7th Mediterranean Conference on Embedded Computing (MECO)* (pp. 1-4). IEEE.
5. Xu, Y., Zhou, X., & Wang, K. (2018, November). Simulation and Modelling of a Vertical a-Si: H PIN Photodiode-Gated LTPS TFT. In *2018 9th International Conference on Computer Aided Design for Thin-Film Transistors (CAD-TFT)*(pp. 1-1). IEEE.
6. Kim, K., & Kuo, Y. (2017). Light Sensing of a-Si: H pin Diode Mechanism of Asymmetric Charge Carrier Transfer. *IEEE Sensors Letters*, *1*(1), 1-4.
7. Mohammed, W. F., & Al-Tikriti, M. N. (2014). Theoretical models and simulation of optoelectronic properties of a-Si-H PIN photosensors. In *Proceedings of the 8th International Conference on Sensing Technology, Liverpool, UK* (pp. 578-582).
8. Jelodarian, P., & Kosarian, A. (2012). Effect of p-layer and i-layer properties on the electrical behaviour of advanced a-Si: H/a-SiGe: H thin film solar cell from numerical modeling prospect. *International Journal of Photo-energy*, *2012*.
9. Boussettine, A. A., Belhadji, Y., & Benmansour, A. (2012). Modeling of tandem solar cell a-Si/a-SiGe using AMPS-1D program. *Energy Procedia*, *18*, 693-700.
10. Zheng, X. X., Zhang, X. D., Yang, S. S., Xu, S. Z., Wei, C. C., Sun, J., ... & Zhao, Y. (2012). Study of a-Si: H/a-Si: H/μc-Si: H PIN type triple junction solar cells in a single chamber system. *Physics Procedia*, *32*, 308-313.